Hindawi
Mathematical Problems in Engineering
Volume 2017, Article ID 2192393, 9 pages
https://doi.org/10.1155/2017/2192393

Research Article

Design of H_2/H_∞ RMPC for Boiler Superheated Steam Temperature Based on Memoryless Feedback Multistep Strategy

Pu Han, Miao Liu, Dongfeng Wang, and Hao Jia

Hebei Engineering Research Center of Simulation & Optimized Control for Power Generation, Department of Automation, North China Electric Power University, Baoding 071003, China

Correspondence should be addressed to Miao Liu; miaoliu_2015@ncepu.edu.cn

Received 13 January 2017; Accepted 14 March 2017; Published 18 April 2017

Academic Editor: Anna Vila

The collection of superheated steam temperature models of a thermal power plant under different loads can be approximated to "multimodel" linear uncertain systems. After transformation, the tracking system was obtained from "multimodel" linear uncertain systems. For this tracking uncertain system, a mixed H_2/H_∞ robust model predictive control (HRMPC) based on a memoryless feedback multistep strategy is proposed. A multistep control strategy combines the advantages of predictive control rolling optimization with memoryless feedback control thoughts. It could effectively decrease the controller optimization parameter and ensure closed-loop system stability, and, at the same time, it also achieved acceptable control performance. Successful application to the superheated steam temperature system of a 300 MW thermal power plant verified the study of the HRMPC-P cascade controller design scheme in terms of feasibility and effectiveness.

1. Introduction

The superheated steam temperature of a thermal power plant directly affects the thermal efficiency, safe operation of the superheated pipe, and the steam turbine equipment. A superheated steam system is characterized by large inertia and a substantial amount of lag [1]. Most power plants continue to adopt a conventional steam temperature control system, such as a cascade PID scheme or double circuit control system with a lead steam temperature differential signal. In recent years, a number of advanced control algorithms were being researched for application in superheated steam temperature systems; these include adaptive fuzzy neural network control [2], adaptive predictive control [3], nonlinear generalized predictive control [4], network cascade control [5], and active disturbance rejection control [6].

Model predictive control (MPC), also known as rolling time control, was first applied to the linear time-invariant (LTI) system [7, 8]. Despite the heavy computational burden incurred in its implementation, MPC is characterized by good robustness, which has been extended to some other important classes of systems, such as distributed systems [9] and nonlinear systems [10]. Its application in industrial contexts is more recent [11]. Uncertainty and disturbance are widespread for the actual system. Using the method of robust control treatment for an uncertain system as reference, robust model predictive control (RMPC) can effectively deal with model uncertainties and disturbance. Furthermore, the controlled system achieves asymptotic stability under the condition of meeting the feasibility. Therefore, as an important branch of model predictive control, RMPC attracts increasing attention [12–14].

Linear matrix inequalities (LMI), just as the name implies, are linear in the matrix variables. Many control problems can be converted into a feasibility problem of an LMI system or a convex optimization problem with LMI constraints [15]. With the development of the LMI toolbox in MATLAB, the LMI approach has been widely used in the field of systems and robust control [16].

Lately, many robust model predictive control algorithms have been proposed [13–17]. Although these algorithms enable the system to approach a stable state, they do not meet the required expectations. Robust tracking controls were investigated for uncertain discrete time systems and application in thermal power plant systems [18–23]. However, the designs were too complicated and some designs had to

undergo online optimization control as independent optimization variables to guarantee the constraint conditions for the control law.

In this paper, we designed a mixed H_2/H_∞ robust model predictive control (HRMPC) based on a memoryless feedback multistep strategy for superheated steam temperature "multimodel" or "multipacket" linear uncertain system of a thermal power plant. Section 2 states the problem to be solved and introduces some standard assumptions. Section 3 discusses the HRMPC method, which adopts a closed-loop multistep control strategy and the memoryless feedback control thought to ensure the stability of the closed loop. At the same time, it could also achieve good control performance. In addition, considering simplified design, robust stability, and practical application, we studied a HRMPC-P cascade controller design scheme with cascade control structure in Section 4. Simulation and experimental results are discussed in Section 5. Lastly, concluding remarks are presented in Section 6.

Preliminaries are as follows:

(1) $\left[\begin{smallmatrix} A & * \\ S & B \end{smallmatrix}\right] = \left[\begin{smallmatrix} A & S^T \\ S & B \end{smallmatrix}\right]$.

(2) Schur Complement Lemma: consider the partitioned matrix

$$A = \begin{bmatrix} A_{11} & A_{12} \\ A_{21} & A_{22} \end{bmatrix}. \tag{1}$$

(a) When A_{11} is nonsingular, $A_{22} - A_{21}A_{11}^{-1}A_{12}$ is called the Schur complement of A_{11} in A.

(b) When A_{22} is nonsingular, $A_{11} - A_{12}A_{22}^{-1}A_{21}$ is called the Schur complement of A_{22} in A.

2. Problem Statement

Consider the following multipacket uncertain systems:

$$\begin{aligned} x(k+1) &= A(k)x(k) + B(k)u(k) + B_\omega \omega(k), \\ y(k) &= Cx(k), \end{aligned} \tag{2}$$

where $x(k) \in R^n$ is the real-time state, $u(k) \in R^m$ is the control input, $y(k) \in R^l$ is the plant output, and $\omega(k) \in R^n$ is the unknown but bounded disturbance. $A(k) \in R^{n\times n}$, $B(k) \in R^{n\times m}$, and

$$\begin{aligned} (A(k), B(k)) \in \Omega &= \Big\{ (A(k), B(k)) \mid (A(k), B(k)) \\ &= \sum_{i=1}^{n_p} \lambda_i (A_i, B_i),\ \lambda_i \geq 0,\ \sum_{i=1}^{n_p} \lambda_i = 1 \Big\}. \end{aligned} \tag{3}$$

(A_i, B_i) represent a state model of the system under a particular operating condition.

In this paper, we consider Euclidean norm bounds and component-wise peak bounds on the input $u(k+i \mid k)$, given, respectively, as

$$\|u(k+i \mid k)\|_2 \leq u_{\max}, \quad k, i \geq 0, \tag{4}$$

$$\left|u_j(k+i \mid k)\right| \leq u_{j,\max}, \quad k, i \geq 0,\ j = 1, 2, \ldots, m \tag{5}$$

with a known bound $u_{\max} > 0$.

Assume that $(A(k), B(k))$ are controllable, and the system external disturbance satisfying (6) is said to be an admissible disturbance

$$\sqrt{\sum_{k=0}^{\infty} w^T(k) w(k)} \leq \varpi \tag{6}$$

with a known upper bound $\varpi > 0$.

The RMPC system reference signal $y_r(k)$ is produced by the following system:

$$\begin{aligned} x_r(k+1) &= A_r x_r(k) + B_r r(k), \\ y_r(k) &= C_r x_r(k), \end{aligned} \tag{7}$$

where $x_r(k)$ are the reference states, $r(k)$ are the expected input values, A_r is the Hurwitz matrix with an appropriate dimension, and B_r, C_r are a constant matrices with an appropriate dimension.

In order to ensure that the state variables of system (2) track the RMPC system reference signal $y_r(k)$, we designed a linear memoryless feedback controller as follows:

$$\begin{aligned} x_c(k+1) &= x_c(k) + x_r(k) - x(k), \\ u(k) &= K^1 x(k) + K^2 x_c(k), \end{aligned} \tag{8}$$

where $x_c(k) \in R^n$ is the controller state and K^1, K^2 are feedback controller gains that need to be solved.

Substituting the memoryless feedback controller (8) into system (2), we have the close-loop system

$$\begin{aligned} x(k+1) &= \left[A(k) + B(k)K^1\right] x(k) + B(k)K^2 x_c(k) \\ &\quad + B_\omega \omega(k), \\ y(k) &= C(k)x(k). \end{aligned} \tag{9}$$

By completing formulas (8) and (9), the tracking system can be obtained

$$\begin{aligned} \overline{x}(k+1) &= \left[\overline{A}(k) + \overline{B}(k)K\right] \overline{x}(k) + \overline{B}_w w(k) \\ &\quad + H x_r(k), \\ y(k) &= \overline{C}(k)\overline{x}(k), \end{aligned} \tag{10}$$

where

$$\begin{aligned} \overline{x}(k) &= \left[x^T(k) \ \ x_c^T(k)\right]^T, \\ \overline{A}(k) &= \begin{bmatrix} A(k) & 0 \\ -I & I \end{bmatrix}, \\ \overline{B}_w(k) &= \left[B_w^T \ \ 0\right]^T, \\ \overline{B}(k) &= \left[B^T(k) \ \ 0\right]^T, \end{aligned}$$

$$K = \begin{bmatrix} K^1 & K^2 \end{bmatrix},$$

$$H = \begin{bmatrix} 0 & I \end{bmatrix}^T,$$

$$\overline{C} = \begin{bmatrix} C & 0 \end{bmatrix},$$

$$\left(\overline{A}(k), \overline{B}(k)\right) \in \overline{\Omega} = \left\{ \left(\overline{A}(k), \overline{B}(k)\right) \mid \left(\overline{A}(k), \overline{B}(k)\right) \right.$$

$$= \sum_{i=1}^{n_p} \lambda_i \left(\begin{bmatrix} A_i(k) & 0 \\ -I & I \end{bmatrix}, \begin{bmatrix} B_i(k) \\ 0 \end{bmatrix} \right)$$

$$\left. = \sum_{i=1}^{n_p} \lambda_i \left(\overline{A}_i(k), \overline{B}_i(k)\right),\ \lambda_i \geq 0,\ \sum_{i=1}^{n_p} \lambda_i = 1 \right\}. \tag{11}$$

Therefore, the tracking system (10) is also a multipacket uncertain system. And the memoryless state feedback control law (8) can be rewritten as

$$u(k) = K\overline{x}(k). \tag{12}$$

Control law (12) is required to make the tracking system (10) meet the following performance index.

(a) H_∞ Performance Index. Given the multiple packet uncertain time-varying discrete system (2) and a positive scalar $\gamma > 0$, design a memoryless state feedback control law $u(k)$ in the form of (12) such that the closed-loop tracking system (10) is asymptotically stable and satisfies

$$\left\| T_{wy} \right\|_\infty \leq \gamma, \tag{13}$$

where T_{wy} is the transfer function from $\omega(k)$ to $y(k)$.

(b) H_2 Performance Index. Given the multiple packet uncertain time-varying discrete system (2) and a scalar $\alpha > 0$, design a memoryless state feedback control law $u(k)$ in the form of (12) such that the output $y(k)$ of the tracking system (10) is asymptotically stable and satisfies

$$\|y\|_2 \equiv \sum_{k=0}^{\infty} y^T(k)\, y(k) \leq \alpha. \tag{14}$$

3. Design of H_2/H_∞ Multistep Robust Predictive Controller

3.1. H_2/H_∞ Performance Index. In order to reduce the conservativeness of the design, the multistep control set $S_0 = \{x \mid x^T Q_0^{-1} x \leq 1\}$ is utilized [11], and the control strategy (15) as the system control law in the future

$$\varepsilon = \left\{ K_0^1, \ldots, K_{N_u-1}^1, K_0^2, \ldots, K_{N_u-1}^2 \right\}, \tag{15}$$

where K_i^1, K_i^2 are predicted feedback gains of the tracking system at sampling time $k+i$. N_u is control horizon.

With respect to the input constraints, we can get

$$\begin{aligned} \left|u_l\right|^2 &= \left|\alpha_l Y_i Q_i^{-1} \overline{x}\right|^2 = \left|\alpha_l Y_i Q_i^{-1/2} Q_i^{-1/2} \overline{x}\right|^2 \\ &\leq \left\|\alpha_l Y_i Q_i^{-1/2}\right\|, \quad l = 1, \ldots, m, \end{aligned} \tag{16}$$

where u_l is the lth element of the control input corresponding to the feedback control gain of K_i^1, K_i^2 and α_l is the lth row of m-dimensional identity matrix.

For this control strategy, we select the Lyapunov function as follows:

$$V(\overline{x}(k+i)) = \overline{x}^T(k+i) P_i \overline{x}(k+i), \quad i = 0, \ldots, N-1, \tag{17}$$

where N is the prediction horizon and the length of N indicates N steps from time k, the predicted output value close to the expected value. $P_i > 0$, when $i > N$, $P_i = P_{N-1}$.

Denote

$$\beta_i(k) = \overline{A}(k) + \overline{B}(k) K + \overline{L} C_0. \tag{18}$$

We can obtain that

$$\begin{aligned} &V(\overline{x}(k+i+1)) - V(\overline{x}(k+i)) = \|\overline{x}(k+i+1)\|_{P_{i+1}}^2 \\ &\quad - \|\overline{x}(k+i)\|_{P_i}^2 = \overline{x}^T(k+i)\, \beta_i^T(k)\, P_{i+1} \beta_i(k)\, \overline{x}(k+i) \\ &\quad + 2\overline{x}^T(k+i)\, \beta_i^T(k)\, P_{i+1} \overline{B}_w w(k+i) + 2\overline{x}^T(k+i) \\ &\quad \cdot \beta_i^T(k)\, P_{i+1} H x_r(k+i) + w^T(k+i) \\ &\quad \cdot \overline{B}_w^T P_{i+1} \overline{B}_w w(k+i) + 2w^T(k+i) \\ &\quad \cdot \overline{B}_w^T P_{i+1} H x_r(k+i) + x_r^T(k+i) H^T P_{i+1} H x_r(k+i) \\ &\quad - \overline{x}^T(k+i) P_i \overline{x}(k+i) + y^T(k+i)\, y(k+i) \\ &\quad - y^T(k+i)\, y(k+i) + \gamma^2 w^T(k+i)\, w(k+i) \\ &\quad - \gamma^2 w^T(k+i)\, w(k+i) \\ &\quad = \left[\overline{x}^T(k+i) \quad v^T(k+i)\right] W_i(k) \\ &\quad \cdot \left[\overline{x}^T(k+i) \quad v^T(k+i)\right]^T - y^T(k+i)\, y(k+i) \\ &\quad + \gamma^2 v^T(k+i)\, v(k+i). \end{aligned} \tag{19}$$

Denote

$$\chi = \beta_i^T(k) P_{i+1} \beta_i(k) - P_i + \overline{C}^T \overline{C}; \tag{20}$$

then

$$W_i(k) = \begin{bmatrix} \chi & \beta_i^T(k) P_{i+1} \overline{B}_w & \beta_i^T(k) P_{i+1} H \\ * & \overline{B}_w^T P_{i+1} \overline{B}_w & \overline{B}_w^T P_{i+1} H \\ * & * & H^T P_{i+1} H \end{bmatrix}. \tag{21}$$

Lemma 1. *For tracking system (10), denote* $K_i = K_i^1 H_1 + K_i^2 H_2$, *where* $H_1 = [I \ \ 0]$, $H_2 = [0 \ \ I]$, *and then a memoryless state feedback control law*

$$K_i = Y_i Q_i^{-1} \tag{22}$$

exists such that $\|T_{wy}\|_\infty \le \gamma$ *if there exist* $\gamma > 0$, $Q_i \in R^{3n\times 3n}$ *and* $Y_i \in R^{3m\times 3n}$ *satisfying*

$$\begin{bmatrix} -Q_i & * & * & * & * \\ 0 & 0 & * & * & * \\ 0 & 0 & -\alpha\gamma^2 I & * & * \\ \overline{A}Q_i + \overline{B}Y_i & \overline{B}_w & H & -Q_{i+1} & * \\ \overline{C}Q_i & 0 & 0 & 0 & -\alpha I \end{bmatrix} \le 0, \tag{23}$$

$$\begin{bmatrix} -1 & * & * \\ \gamma^2\varpi & -\alpha\gamma^2\varpi & * \\ \overline{x}(k) & 0 & -Q_0 \end{bmatrix} \le 0, \tag{24}$$

where $i = 0, \ldots, N-1$.

Proof. We sum both sides of equality (19) from $i = 0$ to $i = \infty$. Actually, when $i > N-1$ the system output is close to the expected value and $\lim_{i\to\infty} V(\overline{x}(k+i)) = 0$; then we obtain the following equation:

$$\begin{aligned} -\overline{x}^T(k) P_k \overline{x}(k) &= \sum_{i=0}^{\infty} \left[-y^T(k+i)\, y(k+i) \right. \\ &\quad \left. + \gamma^2 w^T(k+i)\, w(k+i) \right] \\ &\quad + \sum_{i=0}^{\infty} \left[\overline{x}^T(k+i) \ \ w^T(k+i) \ \ x_r^T(k+i) \right] W_i(k) \\ &\quad \cdot \left[\overline{x}^T(k+i) \ \ w^T(k+i) \ \ x_r^T(k+i) \right]^T. \end{aligned} \tag{25}$$

Equation (25) can be rewritten as

$$\begin{aligned} \sum_{i=0}^{\infty} \left[y^T(k+i)\, y(k+i) \right] &= \overline{x}^T(k) P_k \overline{x}(k) \\ &\quad + \sum_{i=0}^{\infty} \left[\gamma^2 w^T(k+i)\, w(k+i) \right] \\ &\quad + \sum_{i=0}^{\infty} \left[\overline{x}^T(k+i) \ \ w^T(k+i) \ \ x_r^T(k+i) \right] W_i(k) \\ &\quad \cdot \left[\overline{x}^T(k+i) \ \ w^T(k+i) \ \ x_r^T(k+i) \right]^T. \end{aligned} \tag{26}$$

(1) While $x(k) = 0$, the performance index (13) is equivalent to

$$\sum_{i=0}^{\infty} \left[y^T(k+i)\, y(k+i) - \gamma^2 w^T(k+i)\, w(k+i) \right] \le 0. \tag{27}$$

Thus, from (26) it is known that if $W_i(k) \le 0$, then (27) is satisfied. In other words, H_∞ performance index is met.

(2) From (26), if $W_i(k) \le 0$, satisfying the following conditions, then H_2 performance index is met:

$$\sum_{i=0}^{\infty} \left[y^T(k+i)\, y(k+i) \right] \le \overline{x}^T(k) P_0 \overline{x}(k) + \gamma^2 \varpi \le \alpha. \tag{28}$$

For $W_i(k)$, (21) can be written as

$$\begin{aligned} W_i(k) &= \begin{bmatrix} \chi & \beta_i^T(k) P_{i+1} \overline{B}_w & \beta_i^T(k) P_{i+1} H \\ * & \overline{B}_w^T P_{i+1} \overline{B}_w & \overline{B}_w^T P_{i+1} H \\ * & * & H^T P_{i+1} H \end{bmatrix} \\ &= \begin{bmatrix} -P_i & * & * \\ 0 & 0 & * \\ 0 & 0 & -\gamma^2 I \end{bmatrix} + \begin{bmatrix} \overline{C}^T \\ 0 \\ 0 \end{bmatrix} \begin{bmatrix} \overline{C} & 0 & 0 \end{bmatrix} \\ &\quad + \begin{bmatrix} \beta_i^T(k) \\ \overline{B}_w^T \\ H^T \end{bmatrix} P_{i+1} \begin{bmatrix} \beta_i(k) & \overline{B}_w & H \end{bmatrix}. \end{aligned} \tag{29}$$

Further, using the Schur complement in (29), we have

$$\begin{bmatrix} -P_i & * & * & * & * \\ 0 & 0 & * & * & * \\ 0 & 0 & -\gamma^2 I & * & * \\ \beta_i(k) & \overline{B}_w & H & -P_{i+1}^{-1} & * \\ \overline{C} & 0 & 0 & 0 & -I \end{bmatrix} \le 0. \tag{30}$$

Multiply both sides of inequality (30) by using

$$\operatorname{diag}\left\{ \alpha^{1/2} P_i^{-1}, \alpha^{1/2} I, \alpha^{1/2} I, \alpha^{1/2} I, \alpha^{1/2} I \right\}. \tag{31}$$

Denote that $Q_i = \alpha P_i^{-1}$, $K_i = Y_i Q_i^{-1}$; condition (23) can be obtained.

In the same way, using the Schur complement in (28) $\overline{x}^T(k) P_0 \overline{x}(k) + \gamma^2 \varpi \le \alpha$, we have

$$\begin{bmatrix} -\alpha & * & * \\ \gamma^2\varpi & -\gamma^2\varpi & * \\ \overline{x}(k) & 0 & -P_0^{-1} \end{bmatrix} \le 0. \tag{32}$$

Multiplying both sides of inequality (32) by using

$$\operatorname{diag}\left\{ \alpha^{-1/2} I, \alpha^{1/2} I, \alpha^{1/2} I \right\} \tag{33}$$

then condition (24) can be obtained. □

3.2. Constraint Condition. For constraint (5), we have the following lemma.

Lemma 2. *If there exist $Q_i \in R^{3n\times 3n}$ and $Y_i \in R^{3m\times 3n}$, $i = 0, \ldots, N-1$ such that Lemma 1 is established, and there exist symmetric matrices X such that the following inequality is satisfied, then constraint (5) is met*

$$\begin{bmatrix} -X & * \\ Y^T & -Q \end{bmatrix} \le 0, \qquad X_{jj} \le u_{j,\max}^2, \quad j = 1, 2, \ldots, n_m. \tag{34}$$

Proof. At sample time k, consider the Euclidean norm constraint (5).

$$\|u(k+i \mid k)\|_2 \le u_{\max}, \quad k, i \ge 0. \tag{35}$$

Following controller (12), we have

$$\max_{i\ge 0} \|u(k+i \mid k)\|_2^2 = \max_{i\ge 0} \left\|YQ^{-1}\overline{x}(k+i \mid k)\right\|_2^2 \le \max_{z\in\varepsilon} \left\|YQ^{-1}z\right\|_2^2 = \lambda_{\max}\left(Q^{-1/2}Y^TYQ^{-1/2}\right), \tag{36}$$

where $\varepsilon = \{z \mid z^TQ^{-1}z \le 1\} = \{z \mid z^TPz \le \gamma\}$; using the Schur complement, we have

$$\|u(k+i \mid k)\|_2^2 \le u_{\max}^2, \quad i \ge 0. \tag{37}$$

If the inequality is established

$$\begin{bmatrix} -u_{\max}^2 I & * \\ Y^T & -Q \end{bmatrix} \le 0 \tag{38}$$

at sample time k

$$\left|u_j(k+i \mid k)\right| \le u_{j,\max}, \quad i \ge 0, \ \ j = 1, 2, \ldots, m \tag{39}$$

using the Cauchy-Schwarz inequality [24], we have

$$\max_{i\ge 0} \left|u_j(k+i \mid k)\right|^2 = \max_{i\ge 0} \left|\left(YQ^{-1}x(k+i \mid k)\right)_j\right|^2 \le \max_{z\in\varepsilon} \left|\left(YQ^{-1}z\right)_j\right|^2 \le \left|\left(YQ^{-1/2}\right)_j\right|_2^2 = \left(YQ^{-1}Y^T\right)_{jj}. \tag{40}$$

Thus, symmetric matrix X satisfies

$$\begin{bmatrix} -X & * \\ Y^T & -Q \end{bmatrix} \le 0, \qquad X_{jj} \le u_{j,\max}^2, \quad j = 1, 2, \ldots, n_m, \tag{41}$$

where X_{jj} are diagonal elements of matrix X.

In conclusion, for tracking system (10), we have the memoryless feedback multistep H_2/H_∞ robust model predictive control algorithm from Lemmas 1 and 2. At sample time k, solve the following optimization problem:

$$\min_{Q_i, Y_i, X_i, \alpha} \ \alpha \quad \text{Subject to} \quad (23), (24), (34). \tag{42}$$

The current system input of the controller is

$$u(k) = K\overline{x}(k). \tag{43}$$

□

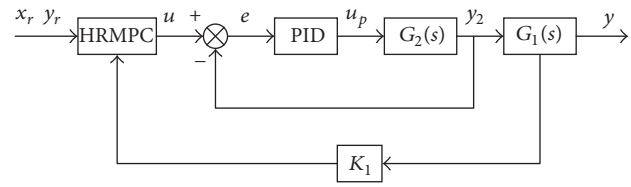

Figure 1: HRMPC-P control structure.

3.3. Robust Stability

Theorem 3. *Consider the multipacket uncertain tracking system (14). If the optimization problem is feasible with the system state $\overline{x}(k)$, then system (14) in close-loop is robustly stable.*

Proof. At sample time k, optimization problem (42) is feasible with the optimal solution

$$\{Q_0, \ldots, Q_{N-1}, Y_0, \ldots, Y_{N-1}, X_0, \ldots, X_{N-1}, \gamma(k)\}. \tag{44}$$

While disturbance exists at sample time $k+1$, the optimization problem (42) has the optimal solution

$$\{Q_1, \ldots, Q_{N-1}, Q_{N-1}, Y_1, \ldots, Y_{N-1}, Y_{N-1}, X_1, \ldots, X_{N-1}, X_{N-1}, \gamma^*(k)\}, \tag{45}$$

where $\gamma(k+1) = \gamma^*(k)$, and by the principle of optimization, we have

$$\gamma^*(k) \ge \gamma(k+1) \ge \gamma^*(k+1). \tag{46}$$

When disturbance disappears, due to the fact that $W_i(k) \le 0$, $V(k+1) < V(k)$, it means that $V(k)$ will decay to 0. Thus, the closed-loop system has robust stability. □

4. HRMPC-P Cascade Controller Design

The optimization goal of the inner loop is to quickly eliminate interference from the spraying system or burning system, and the optimization goal does not require difference. As a result, the proportional controller is often used in the inner loop, which is regarded as a quick follow-up system. In this paper, we study HRMPC-P controller design with a cascade control structure by considering a simplified design, robust stability, and practical application. A proportional controller is adopted for the inner loop. The HRMPC-P cascade control structure is as shown in Figure 1.

Assume that the secondary superheated transfer functions are known, including both the leading and inertia segments. The HRMPC-P cascade control design steps are as follows:

(1) Select appropriate rolling optimization steps N, control horizon N_u, and γ. The feasible regions of the controller broaden as N_u increases [11].

(2) Optimize the inner loop PID controller; in this work, the proportional controller simply needs to optimize the proportional gain δ.

(3) Set expectations r and the reference system.

Table 1: Discrete state space model.

	Leading segment		Inertia segment	
	A_2	B_2	A	B
180 MW	$\begin{bmatrix} 0.9536 & 0 & 0 & 0 \\ 0.0464 & 0.9536 & 0 & 0 \\ 0 & 0.0464 & 0.9536 & 0 \\ 0 & 0 & 0.0464 & 0.95362 \end{bmatrix}$	$\begin{bmatrix} -0.0464 \\ 0 \\ 0 \\ 0 \end{bmatrix}$	$\begin{bmatrix} 0.9627 & 0 & 0 & 0 \\ 0.0373 & 0.927 & 0 & 0 \\ 0 & 0.0373 & 0.9627 & 0 \\ 0 & 0 & 0.0373 & 0.9627 \end{bmatrix}$	$\begin{bmatrix} 0.0447 \\ 0 \\ 0 \\ 0 \end{bmatrix}$
250 MW	$\begin{bmatrix} 0.9612 & 0 & 0 & 0 \\ 0.0388 & 0.9612 & 0 & 0 \\ 0 & 0.0388 & 0.9612 & 0 \\ 0 & 0 & 0.0388 & 0.9612 \end{bmatrix}$	$\begin{bmatrix} -0.0388 \\ 0 \\ 0 \\ 0 \end{bmatrix}$	$\begin{bmatrix} 0.9732 & 0 & 0 & 0 \\ 0.0268 & 0.9732 & 0 & 0 \\ 0 & 0.0268 & 0.9732 & 0 \\ 0 & 0 & 0.0268 & 0.9732 \end{bmatrix}$	$\begin{bmatrix} 0.0268 \\ 0 \\ 0 \\ 0 \end{bmatrix}$

(4) At sample time k, when $i = 0$, solve optimization problem (42), and obtain the optimal solution

$$\{Q_0, \ldots, Q_{N-1}, Y_0, \ldots, Y_{N-1}, X_0, \ldots, X_{N-1}, \gamma(k)\}. \quad (47)$$

(5) $i = i+1, \ldots$, until $i = N$, and obtain the corresponding optimal solution

$$\{Q_1, \ldots, Q_{N-1}, Q_{N-1}, Y_1, \ldots, Y_{N-1}, Y_{N-1}, X_1, \ldots, X_{N-1}, X_{N-1}, \gamma^*(k)\}. \quad (48)$$

(6) Determine the current moment controller output

$$u(k) = K_k \overline{x}(k). \quad (49)$$

(7) Taking $u(k)$ into the inner loop discrete state space model (50), we have $y_2(k)$

$$x_2(k+1) = A_2(k) x_2(k) + B_2(k) u_p(k), \quad y_2(k) = C x_2(k), \quad (50)$$

where $x_2(k)$ is the leading segment state, $u_p(k)$ is the proportional control output, $y_2(k)$ is the leading segment output.

(8) Taking $y_2(k)$ into the tracking system (10), we have the state $\overline{x}(k+1)$.

(9) Make $k = k+1$, jump to Step (4).

5. Simulation

Choose two secondary superheated system transfer functions under different loads of 180 MW and 250 MW of a 300 MW power unit [21]. Design the controller to use the method discussed in Sections 4 and 5.

$$G_1(s) = \frac{-1}{(20s+1)} \frac{1.2}{(25s+1)^4} \ (^\circ\mathrm{C}/\%), \quad G_2(s) = \frac{-1}{(24s+1)} \frac{1}{(35s+1)^4} \ (^\circ\mathrm{C}/\%). \quad (51)$$

The first part is a leading segment transfer function and the last part is the inertia segment transfer function for each transfer function.

Using a sampling time $T = 0.95$ s, convert the transfer function mode into discrete state space mode. After discretization, the leading segment and the inertia segment are as in Table 1.

In each state $\|\omega(k)\|_2^2 \le 0.01$, $\varpi = 0.5$,

$$C = \begin{bmatrix} 0 & 0 & 0 & 1 \end{bmatrix}, \quad B_w = \begin{bmatrix} 0 & 0 & 0 & 0.1 \end{bmatrix}^T, \quad A_r = \begin{bmatrix} 0.827 & 0 & 0 & 0 \\ 0.173 & 0.827 & 0 & 0 \\ 0 & 0.173 & 0.827 & 0 \\ 0 & 0 & 0.173 & 0.827 \end{bmatrix}, \quad (52)$$

$$B_r = \begin{bmatrix} 0.173 & 0 & 0 & 0 \end{bmatrix}^T, \quad C_r = \begin{bmatrix} 0 & 0 & 0 & 1 \end{bmatrix}.$$

The step responses of the system with different values of γ are shown in Figure 2. Choose the transfer function $G_1(s)$ as an example, set the value of $\gamma = 0.1$ and $\gamma = 2$, and we have the step responses of the system. As is shown in the figure, the ability to restrain the interference of the system is increased with the decrease of γ.

The tracking performance of different controllers is shown in Figure 5. Choose the transfer function $G_1(s)$ as an example. We compared the control quality of HRMPC-P cascade control with the conventional cascade PID control (PID-P) and dynamic matrix control [6] (DMC-P) through the system output tracking situation. The control laws and control structures are illustrated as follows.

(1) PID Controller

$$u_{\mathrm{PID}}(t) = K_P e(t) + K_i \int e(t)\, dt + K_d \frac{de(t)}{dt}, \quad e(t) = y(t) - y_r(t), \quad (53)$$

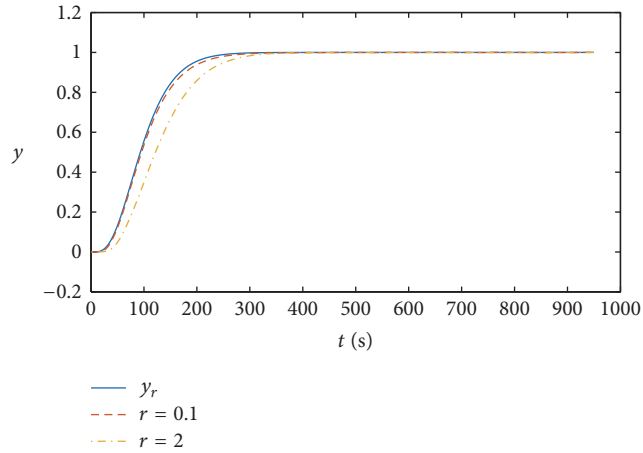

Figure 2: Step responses of the system for different values of γ.

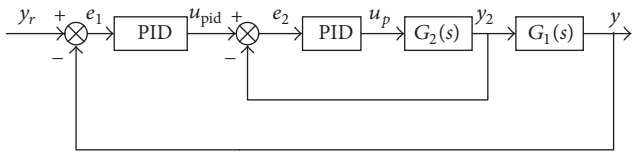

Figure 3: PID-P control structure.

where K_P, K_i, and K_d all nonnegative, denoting the coefficients for the proportional, integral, and derivative terms; $e(t)$ is the difference between a desired set point and a measured process variable. The PID-P control structure is shown in Figure 3.

(2) DMC Controller

$$u_{\mathrm{DMC}}(k) = u_{\mathrm{DMC}}(k-1) + \Delta u_{\mathrm{DMC}}(k)\, d_i, \quad \Delta u_{\mathrm{DMC}}(k) = \left(G^T Q G + \lambda\right)^{-1} G^T Q \left[Y_r(k+1) - G_0 U(k-1) - he(k)\right], \tag{54}$$

where G is dynamic matrix; G_0 is process matrix which is composed of dynamic coefficients; Q and h are the weighting matrices. d_i means the ith row of $\Delta u_{\mathrm{DMC}}(k)$, if the current moment $i = 1$. The DMC-P control structure is shown in Figure 4.

(3) HRMPC-P Controller. The control law and control structure refer to (12) and Figure 1.

As is shown in Figure 5, the HRMPC-P cascade control enables the system to have good tracking performance such that the system output can meet the expectations faster. The inputs of the different controllers are shown in Figure 6(a). The inputs of HRMPC controller, DMC controller, and PID controller, respectively, are system states, control increment, and the difference between desired set points and measured process variables. The outputs of the different controllers are shown in Figure 6(b). The HRMPC-P controller has a smaller output range and faster adjusting speed and can complete the adjustment in about 200 s.

As is shown in Figure 7, the load command changes from 180 MW to 250 MW when $t = 1000$ s. Under this condition, when $t = 1000$ s the system model translates from $G_1(s)$ to $G_2(s)$. The robustness of different controllers is shown in Figure 8. HRMPC-P cascade control still has an enhanced tracking effect, which can quickly adjust the system to the expected value while the system changes. Thus, HRMPC-P cascade control structure has stronger robustness.

Figure 9 shows the output of different controllers while the load command changes. The HRMPC-P controller also has a smaller output range and faster adjusting speed. The variation tendency of HRMPC controller gains K^1 and K^2 is shown in Figure 10. The variation range of these two gain groups is small, and they adjust quickly as well.

6. Concluding Remarks

This paper presents a design strategy for a memoryless feedback multistep H_2/H_∞ RMPC controller for the superheated steam temperature of a thermal power unit. In this study, the collection of superheated steam temperature model under different load is approximated to "multimodel" linear uncertain systems. After transformation, the tracking system is obtained. Then through deduction, we have the HRMPC control flow. Moreover, successful application of the proposed HRMPC-P cascade control scheme to the superheated steam temperature system of a thermal power plant and improved control qualities are achieved. The HRMPC-P cascade control scheme is able to adapt to the whole operating range of the superheated steam temperature system of thermal power plants. Moreover, the decrease in the number of controller

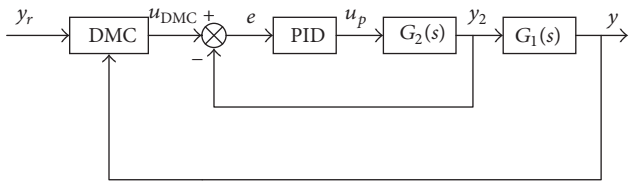

Figure 4: DMC-P control structure.

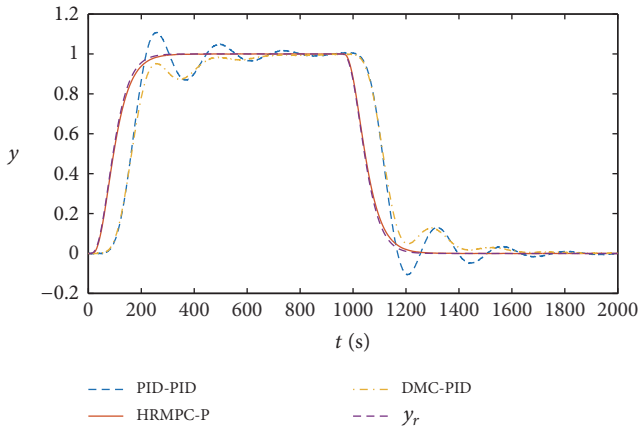

Figure 5: Tracking performance of different controllers.

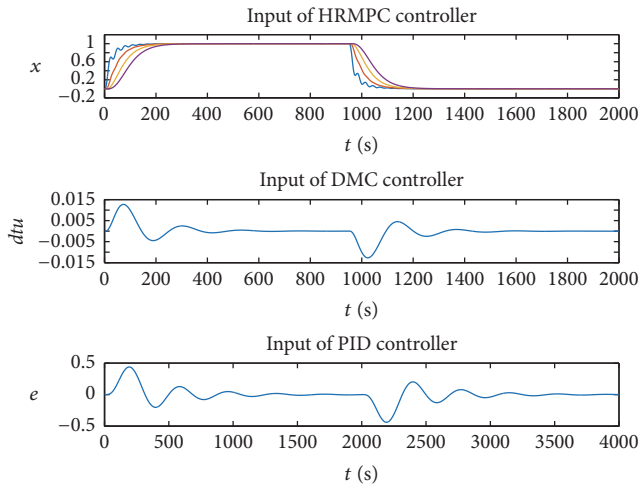

(a) Input of different controllers

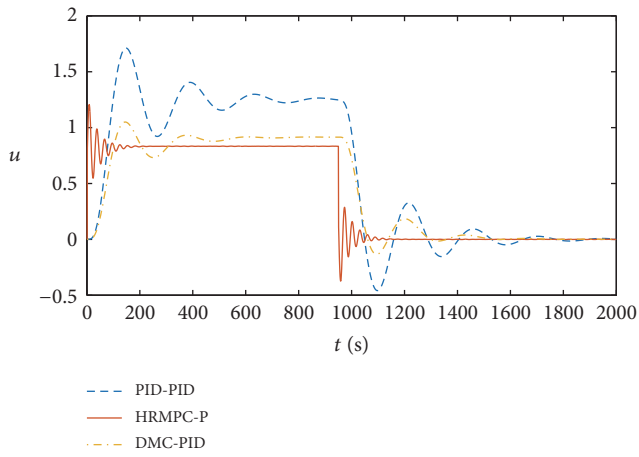

(b) Output of different controllers

Figure 6: Input and output of different controllers.

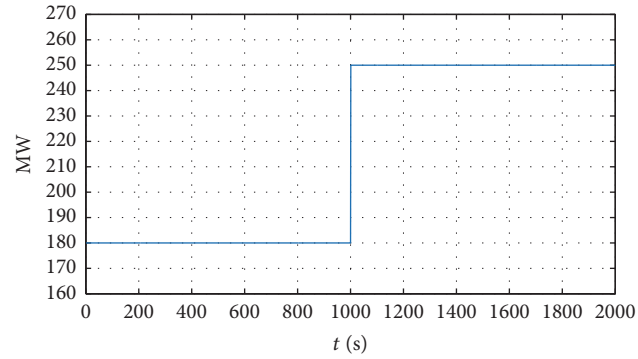

Figure 7: Load command.

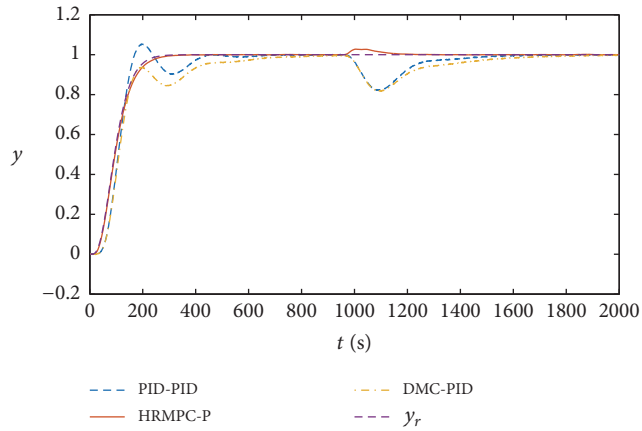

Figure 8: Robustness of different controllers.

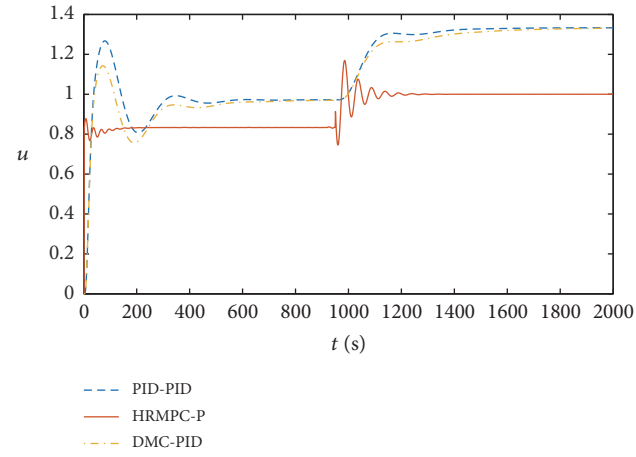

Figure 9: Output of different controllers.

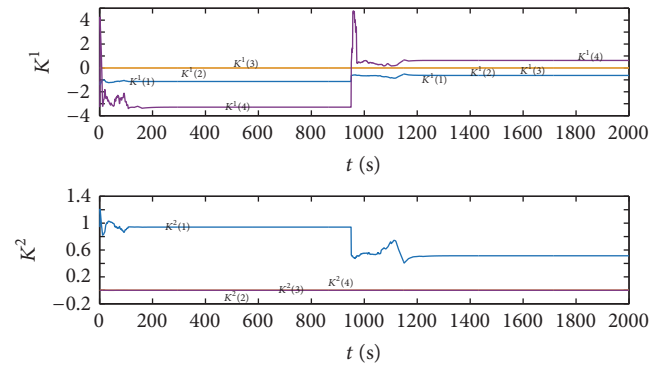

Figure 10: The HRMPC controller gain.

parameters may serve as a reference for actual engineering projects.

Conflicts of Interest

The authors declare that they have no conflicts of interest.

Acknowledgments

This research was supported by the National Natural Fund of China under Grant no. 71471060 and the Coal Based Key Scientific and Technological Project of Shanxi Province, China, under Grant no. MD2014-03-06-02.

References

[1] D. Wang and S. Yuan, "Identification of LPV model for superheated steam temperature system using A-QPSO," *Simulation Modelling Practice and Theory*, vol. 69, pp. 1–13, 2016.

[2] X. Dong, Y. Zhao, H. R. Karimi, and P. Shi, "Adaptive variable structure fuzzy neural identification and control for a class of MIMO nonlinear system," *Journal of the Franklin Institute*, vol. 350, no. 5, pp. 1221–1247, 2013.

[3] W. Yao, H. Sun, J. Wen, and S. Cheng, "An adaptive predictive PI control system of super-heated steam temperature based on Laguerre model," *Proceedings of the Chinese Society of Electrical Engineering*, vol. 32, no. 5, pp. 119–125, 2012.

[4] B. Xiao, X. Zhang, and X. Dong, "Superheated steam temperature control research of the improved implicit generalized predictive algorithm based on the soft coefficient matrix," *Journal of Computational and Theoretical Nanoscience*, vol. 9, no. 10, pp. 1733–1740, 2012.

[5] J. Zhang, S. Zhou, M. Ren, and H. Yue, "Adaptive neural network cascade control system with entropy-based design," *IET Control Theory & Applications*, vol. 10, no. 10, pp. 1151–1160, 2016.

[6] G. Liang, W. Li, and Z. Li, "Control of superheated steam temperature in large-capacity generation units based on active disturbance rejection method and distributed control system," *Control Engineering Practice*, vol. 21, no. 3, pp. 268–285, 2013.

[7] F. Blanchini, D. Casagrande, G. Giordano, and U. Viaro, "Robust constrained model predictive control of fast electromechanical systems," *Journal of the Franklin Institute*, vol. 353, no. 9, pp. 2087–2103, 2016.

[8] Y. Ding, Z. Xu, J. Zhao, and Z. Shao, "Fast model predictive control combining offline method and online optimization with K-D tree," *Mathematical Problems in Engineering*, vol. 2015, Article ID 982041, 10 pages, 2015.

[9] S. Yan, F. Xiaosheng, and D. Qingda, "Mixed H_2/H_∞ distributed robust model predictive control for polytopic uncertain systems subject to actuator saturation and missing measurements," *International Journal of Systems Science*, vol. 47, no. 4, pp. 777–790, 2016.

[10] G. V. Raffo, M. G. Ortega, and F. R. Rubio, "An integral predictive/nonlinear H_∞ control structure for a quadrotor helicopter," *Automatica*, vol. 46, no. 1, pp. 29–39, 2010.

[11] H. Han and J. Qiao, "Nonlinear model-predictive control for industrial processes: an application to wastewater treatment process," *IEEE Transactions on Industrial Electronics*, vol. 61, no. 4, pp. 1970–1982, 2014.

[12] D. Q. Mayne, "Model predictive control: recent developments and future promise," *Automatica*, vol. 50, no. 12, pp. 2967–2986, 2014.

[13] H. Li and Y. Shi, "Event-triggered robust model predictive control of continuous-time nonlinear systems," *Automatica*, vol. 50, no. 5, pp. 1507–1513, 2014.

[14] A. J. Del Real, A. Arce, and C. Bordons, "Combined environmental and economic dispatch of smart grids using distributed model predictive control," *International Journal of Electrical Power and Energy Systems*, vol. 54, pp. 65–76, 2014.

[15] M. J. Park, O. M. Kwon, and E. J. Cha, "On stability analysis for generalized neural networks with time-varying delays," *Mathematical Problems in Engineering*, vol. 2015, Article ID 387805, 11 pages, 2015.

[16] R. Rao, X. Wang, and S. Zhong, "LMI-based stability criterion for impulsive delays markovian jumping time-delays reaction-diffusion BAM neural networks via gronwall-bellman-type impulsive integral inequality," *Mathematical Problems in Engineering*, vol. 2015, Article ID 185854, 11 pages, 2015.

[17] H. He, D. Li, and X. Yugeng, "On design of mixed H_2/H_∞ RMPC based on multi-step control strategy," *Acta Automatica Sinica*, vol. 38, no. 6, pp. 944–950, 2012.

[18] J. Ding, B. Cichy, K. Galkowski, E. Rogers, and H. Yang, "Parameter-dependent Lyapunov function-based robust iterative learning control for discrete systems with actuator faults," *International Journal of Adaptive Control and Signal Processing*, vol. 30, no. 12, pp. 1714–1732, 2016.

[19] T. Zhongliang, G. S. Sam, T. K. Peng, and H. Wei, "Robust adaptive neural tracking control for a class of perturbed uncertain nonlinear systems with state constraints," *IEEE Transactions on Systems Man Cybernetics-Systems*, vol. 46, no. 12, pp. 1618–1629, 2016.

[20] M. Yu, D. Huang, and W. He, "Robust adaptive iterative learning control for discrete-time nonlinear systems with both parametric and nonparametric uncertainties," *International Journal of Adaptive Control and Signal Processing*, vol. 30, no. 7, pp. 972–985, 2016.

[21] C.-Q. Zhang, F. Yang, J.-Z. Xue, and Y.-X. Huang, "Design of the H_∞ performance state observer for the boiler steam temperature control," *Proceedings of the Chinese Society of Electrical Engineering*, vol. 26, no. 14, pp. 109–113, 2006.

[22] W. Jiang, H.-l. Wang, J.-h. Lu, W.-w. Qin, and G.-b. Cai, "Nonfragile robust model predictive control for uncertain constrained systems with time-delay compensation," *Mathematical Problems in Engineering*, vol. 2016, Article ID 1945964, 14 pages, 2016.

[23] Z. Guoqiang and L. Jinkun, "Neural network-based adaptive backstepping control for hypersonic flight vehicles with prescribed tracking performance," *Mathematical Problems in Engineering*, vol. 2015, Article ID 591789, 10 pages, 2015.

[24] M. V. Kothare, V. Balakrishnan, and M. Morari, "Robust constrained model predictive control using linear matrix inequalities," *Automatica*, vol. 32, no. 10, pp. 1361–1379, 1996.